http://dx.doi.org/10.1590/2179-10742016v15i3612

A correction method for the analytical model in Raman amplifiers systems based on energy conservation assumption

Thiago V. N. Coelho, A. Bessa dos Santos, Marco A. Jucá, Luiz C. C. Jr.
Federal University of Juiz de Fora (UFJF), Electrical Circuit Department, Juiz de Fora – MG, Brazil
thiago.coelho@ufjf.edu.br
Maria J. Pontes[a], Andres P. L.Barbero[b]
[a]Federal University of Espírito Santo (UFES), Electrical Engineering Department, Vitoria – ES, Brazil
[b]Fluminense Federal University (UFF), Telecommunications Egineering Department, Niterói – RJ, Brazil

***Abstract*— This paper presents a modification for the already consolidated analytical model that calculates the gain and ripple in multi-pump Raman amplifiers by considering energy conservation. The original analytical model precisely computes the pump-pump interaction to the C- and L-band for a WDM input signal. However, when this method is used to amplify a large bandwidth, as the entire C and a part of the L band, the increase in the number of pump lasers impacts the obtained results. The error, if compared with results obtained by a numerical method, becomes significant. An analysis in terms of energy is proposed to minimize the discrepancy between analytical and numerical results. An improvement is observed to the gain results.**

***Index Terms*—** Raman amplifier, numerical model, analytical model, energy conservation

I. INTRODUCTION

Long distance optical networks are responsible for creating a demand for broadband optical amplification technologies. These technologies must meet the demands for boosting the signal to compensate the signal attenuation in the silica optical fiber along the transmission length. Therefore, the system capacity will increase, replacing the electrical regenerators and lowering the deployment and maintenance costs for long distance optical transmission networks [1, 2].

Raman amplifiers dynamics are based on the nonlinear effect observed in optical fibers known as Stimulated Raman Scattering (SRS). Their main characteristic is the energy transfer from one or more high power pump wavelengths to the signals wavelengths. In comparison with Erbium doped fiber amplifiers (EDFA), Raman amplifiers do not need specialized or doped fibers, using the single mode fiber (SMF) as optical gain medium and have a much larger spectrum that can be tuned selecting different pump parameters as the number and position of the pumps and the intensity of each one of them.

Other important application for Raman amplifiers is the remote operation, by several kilometers, in optical fiber sensors [3]. In particular, the tuned bandwidth characteristic in Raman amplifiers is useful to perform measurements in multiplexed sensor architectures [4].

Raman amplifiers can operate as distributed amplifiers when applied in the SMF optical fiber, since the amplification process occurs in a large fiber length compared to amplification schemes applying

Brazilian Microwave and Optoelectronics Society-SBMO *received 10 Mar 2016; for review 17 Mar 2016; accepted 7 July 2016*
Brazilian Society of Electromagnetism-SBMag *ISSN 2179-1074*

http://dx.doi.org/10.1590/2179-10742016v15i3612

doped optical fibers. Distributed amplifiers have the advantage of increasing the noise figure in comparison with the EDFA technology, increasing optical signal-to-noise ratio (OSNR) and allowing a better power distribution along the fiber, causing lower impact due to nonlinearities.

Other classification takes into account the different pump architectures. The co-propagation scheme occurs when the pump is coupled in the same propagation direction of the signal to be amplified, whereas the counter-propagation scheme is related to counter-propagation direction between the signal and the pump optical beam. The bi-directional configuration combines both architectures cited before.

A co-propagating system shows larger optical intensity gain, but suffers with highest power instability transfer from the laser source to the signal. Another important factor is that the increase in the power inserted into the fiber can lead to unwanted nonlinear effects in the signal wavelength.

The counter-propagating setup shows lower gain than the co-propagating scheme. However, the transfer of instability noise from the optical pump to the optical signal is lower, the gain dependence with the polarization state is less important and the amplification occurs when the signal is not excessively intense; thus, the problem of non-linear effect is less significant. This latter characteristic can also be a negative factor because the signal to be amplified can be at the same level of the noise floor. The bi-directional configuration combines the characteristics of co-propagating and counter-propagating [5-7].

A numerical model was implemented by Cani et al [8] based on coupled differential equations that describe the spatial propagation of multi-pumps and multi-signals in a Raman amplification environment which include all the meaningful physical parameters for the performance analysis in the continuous wave (CW) regime. However, this model with a large number of pumps and signals could demand high costs in computational resources.

An analytical model was proposed by Cani et al., decoupling the differential equations. This model, already validated by measurement results in [8] was built taking into account some simplifications and because of that the power budget of the simulated link can yield unrealistic results for a large number of pumps and signals.

This work proposes a modification in the analytical method to correct the power budget that allows approximating the results of the gain spectrum to the numerical results, mainly for the case of multi-pumps. This will permit the use of this method in optimization techniques to ensure the optimal design of the gain bandwidth for broadband optical networks.

II. MATHEMATICAL MODEL

The Raman amplifier technology is based on a nonlinear effect called Stimulated Raman Scattering (SRS), responsible for transferring energy between different wavelength optical signals based on phase matching conditions. Its main characteristic is the energy transfer from one or more pump wavelengths to the wavelength signals that will be amplified [9].

  ISSN 2179-1074

http://dx.doi.org/10.1590/2179-10742016v15i3612

Figure 1 shows a scheme of the interaction of the incident photons, at frequency υ_0, with silica molecules that is responsible for its absorption by a vibrational state of the matter. Therefore, the incident photons lose energy to the matter and will be scattered in a lower frequency; or in a higher wavelength. These scattered photons at higher wavelengths are called Stokes photons. Meanwhile, if the vibrational state is already excited, due thermal excitation for instance, and the silica molecules return to the ground state after the absorption, the scattering will occur in higher frequency; or in lower wavelength, so these scattered photons at lower wavelengths are called Anti-Stokes photons. The Raman amplification scheme relies only in stokes photons interactions because they are dominant for regular environmental temperatures.

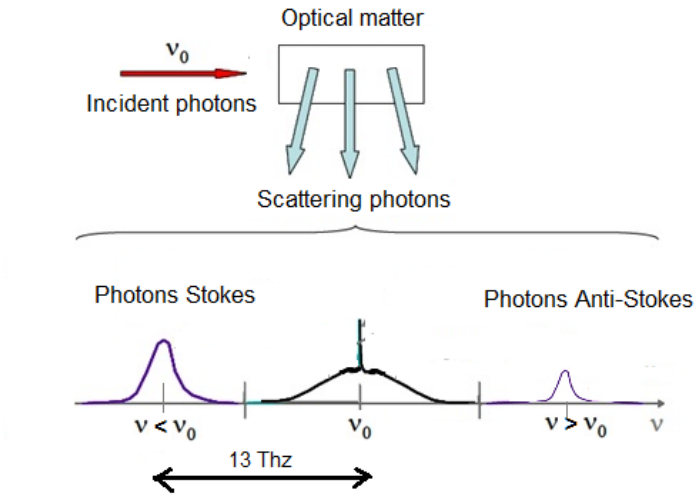

Fig. 1. Scheme of Stokes and Anti-Stokes interaction for Raman amplifiers.

The Raman gain spectrum has a bandwidth of 40 THz with a gain peak around 13 THz away from the pump wavelength. For signal wavelengths to be amplified at 1550 nm, the peak gain is located around 100 nm away from the pump wavelength [10].

Figure 2 shows the schematic for Raman amplification systems that comprises of one or more optical pumps that will be launched in the optical fiber length in three different configurations: co-propagation scheme (a) or counter propagation scheme (b) related to the optical signal direction. The third configuration launches the optical pumps in both directions.

  ISSN 2179-1074

http://dx.doi.org/10.1590/2179-10742016v15i3612

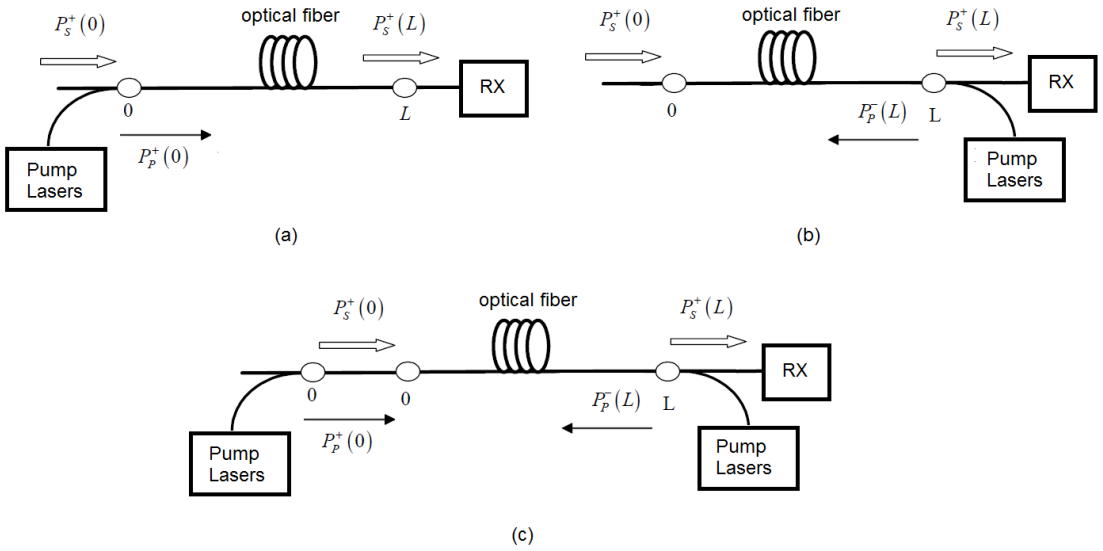

Fig. 2.Raman amplification systems with different pump configurations.

A. Numerical Model

The following numerical model applied in this work was proposed by Cani et.al [8] and taking into account several effects like the single and double Rayleigh scattering, the amplified spontaneous emission (ASE) noise, polarization effects, signal and pump attenuation and the interaction between different pumps, between pumps and signals and between different signals [6, 7].

$$\frac{dP_\nu^\pm}{dz} = \mp\alpha_\nu P_\nu^\pm \pm \varepsilon_\nu P_\nu^\mp$$
$$\pm \mathrm{P}_\nu^\pm \sum_{\mu>\nu} \frac{\mathrm{C}_{\mathrm{R}\mu\nu}}{\Gamma}\left(P_\mu^+ + P_\mu^-\right)$$
$$\pm 2h\nu B_e \sum_{\mu>\nu} \frac{C_{R\mu\nu}}{\Gamma}\left(P_\mu^+ + P_\mu^-\right)\left(1+\eta(T)\right)$$
$$\mp \mathrm{P}_\nu^\pm \sum_{\mu<\nu} \frac{\omega_\nu}{\omega_\mu}\frac{\mathrm{C}_{\mathrm{R}\mu\nu}}{\Gamma}\left(P_\mu^+ + P_\mu^-\right)$$
$$\mp \mathrm{P}_\nu^\pm \sum_{\mu<\nu} \frac{\omega_\nu}{\omega_\mu}\frac{\mathrm{C}_{\mathrm{R}\mu\nu}}{\Gamma}\left(P_\mu^+ + P_\mu^-\right)\left(1+\eta(T)\right)4h\mu B_e \qquad (1)$$

where P_μ, P_ν, α_μ e α_ν are the power and attenuation coefficients at frequencies μ and ν respectively. The superscripts + and – indicate, respectively, the forward and backward propagation in the z axis direction, $C_{R\mu\nu}$ is the Raman gain efficiency between the frequencies μ and ν, Γ is the polarization factor and takes a value 1 if the polarizations are preserved and 2 when the polarizations are not maintained, ε_ν is the Rayleigh scattering coefficient and B_e is the noise bandwidth considered.

  ISSN 2179-1074

http://dx.doi.org/10.1590/2179-10742016v15i3612

B. Analytical Model

The analytical model proposed by Cani et al. [8] obtained with some simplification of the differential equations in Eq.(1) was applied to achieve a model with low computational costs, capable of being applied at optimization techniques to facilitate the choice of the pumps parameters in Raman amplifiers systems. This model approximates to the solutions of the numerical model under certain conditions.

The simplifications applied for the analytical model were to neglect the effect of the double Rayleigh scattering, the ASE noise and the pump depletion by the signal. Other important factor to accomplish the simplification for the analytical solution was considering the attenuation coefficient of the pumps as being the same, so the mean value of them was considered [8, 9]. Therefore, the spatial propagation for three different pumps under counter-propagation direction, with μ > η > σ, can be represented by:

$$\frac{dP_{\mu}^{-}}{dz} = \alpha P_{\mu}^{-} + \frac{\omega_{\mu} C_{R\eta\mu} P_{\eta}^{-}}{\omega_{\eta} \Gamma} P_{\mu}^{-} + \frac{\omega_{\mu} C_{R\sigma\mu} P_{\sigma}^{-}}{\omega_{\sigma} \Gamma} P_{\mu}^{-} \tag{2}$$

$$\frac{dP_{\eta}^{-}}{dz} = \alpha P_{\eta}^{-} - \frac{C_{R\eta\mu} P_{\mu}^{-}}{\Gamma} P_{\eta}^{-} + \frac{\omega_{\eta} C_{R\sigma\eta} P_{\sigma}^{-}}{\omega_{\sigma} \Gamma} P_{\eta}^{-} \tag{3}$$

$$\frac{dP_{\sigma}^{-}}{dz} = P_{\sigma}^{-} - \frac{C_{R\sigma\mu} P_{\mu}^{-}}{\Gamma} P_{\sigma}^{-} - \frac{C_{R\sigma\eta} P_{\eta}^{-}}{\Gamma} P_{\sigma}^{-} \tag{4}$$

To solve this system of coupled equations, eqs.2-4, two iterations were performed, each one with three steps. In the first iteration, two equations are decoupled in each step. Thus, in this iteration two pumps have no interactions with other pumps and the third contains the pumping loss or gain due the relationship with the other pumps [7]. The solution for the first iteration of the systems equations is described as follows,

$$P_{\sigma}^{(1)-}(z) = P_{\sigma}^{-}(L) exp[-\alpha(L-z)] \; exp\left[\frac{1-exp[-\alpha(L-z)]}{\Gamma\alpha}\left(C_{R\sigma\mu} P_{\mu}^{-}(L) + C_{R\sigma\eta} P_{\eta}^{-}(L)\right)\right] \tag{5}$$

$$P_{\eta}^{(1)-}(z) = P_{\eta}^{-}(L) exp[-\alpha(L-z)] exp\left[\frac{1-exp[-\alpha(L-z)]}{\Gamma\alpha}\left(C_{R\eta\mu} P_{\mu}^{-}(L) - \frac{\omega_{\eta} C_{R\sigma\eta}}{\omega_{\sigma}} P_{\eta}^{-}(L)\right)\right] \tag{6}$$

$$P_{\mu}^{(1)-}(z) = P_{\mu}^{-}(L) exp[-\alpha(L-z)]$$
$$exp\left[\frac{1-exp[-\alpha(L-z)]}{\Gamma\alpha}\left(-\frac{\omega_{\mu} C_{R\eta\mu}}{\omega_{\eta}} P_{\eta}^{-}(L) - \frac{\omega_{\mu} C_{R\sigma\mu}}{\omega_{\sigma}} P_{\sigma}^{-}(L)\right)\right] \tag{7}$$

The analytical model does not take into account energy conservation among the pumps. This happens because at each step, the solution of the first iteration considers only the pump-pump interaction in only one equation. In order to minimize this effect, a second iteration was performed

  ISSN 2179-1074

http://dx.doi.org/10.1590/2179-10742016v15i3612

applying the first iteration solution, eqs. 5-7, in the eqs. 2-4. The second iteration solution is achieved and its generalization allows describing a model for n-pumps and n-signals, eqs. 8-9 [8].

$$P_{\mu}^{(2)-}(z) = P_{\sigma}^{-}(L)exp[-\alpha(L-z)]$$

$$exp\left[\sum_{\sigma<\mu}\left[-\omega_{\mu}C_{R\mu\sigma}P_{\mu}^{-}(L)\frac{1-exp\left[\frac{-(1-exp[-\alpha(L-z)])}{\Gamma\alpha}\Psi\right]}{\omega_{\sigma}\Psi}\right]\right]$$

$$exp\left[\sum_{\sigma>\mu}\left[C_{R\mu\sigma}P_{\mu}^{-}(L)\frac{1-exp\left[\frac{-(1-exp[-\alpha(L-z)])}{\Gamma\alpha}\Psi\right]}{\Psi}\right]\right] \quad (8)$$

where:

$$\Psi = \left(\sum_{\eta>\sigma} -C_{R\sigma\eta}P_{\eta}^{-}(L) + \sum_{\eta<\sigma}\omega_{\sigma}C_{R\sigma\eta}P_{\eta}^{-}(L)/\omega_{\eta}\right)$$

The signal gain ($G_{anal,v}(z)$) is calculated by the equation:

$$G_{anal,v}(z) = \exp[-\propto_{v} z]exp\left[\int_{0}^{z}\sum_{\mu=1}^{N_b}\frac{C_{R\mu v}P_{\mu}^{-}(\varepsilon)}{\Gamma}d\epsilon\right] \quad (9)$$

Therefore, the analytical model describes the propagation and interaction between pumps and thereafter computes the signal gain, provided by these pumps, as represented by the eq. 9.

In this case, the pump depletion by the signal can be disregarded. Other important factor to apply this model can be observed when the input signal has high enough power to neglect the ASE influence, this happens when the signal has more than -30 dBm. [8].

C. Corrected Model

As mentioned before, the analytical model is the result of an approach made disregarding the pump depletion by the signal, the double Rayleigh scattering and the ASE of the amplifier. These approaches are effective when working in small signal regime and a few number of pump lasers. Therefore, this solution suffers with this simplification not taking into account energy preservation in the process.

However, when the amplifying system covers a large bandwidth, the C+L optical bandwidth for instance, the number of pumps to accomplish that goal can be large enough to make the results of the analytical model not correspond to real values. Moreover, in this scenario a certain number of pumps will be responsible for amplifying other pumps and the simplification of not considering the depletion of the pump by another pump will be responsible for a large error in the analytical model results.

In this work an analysis in terms of energy conservation was performed. It was considered that all energy loss or gain comes from the interaction between pumps, with the exception of power loss due

received 10 Mar 2016; for review 17 Mar 2016; accepted 7 July 2016

ISSN 2179-1074

http://dx.doi.org/10.1590/2179-10742016v15i3612

the optical fiber attenuation. Therefore, the total energy inserted into the optical fiber can be calculated by the sum of all pump powers that propagate over the optical fiber without considering the interaction between them.

Thus, the total power difference between the energy conservation assumption and the analytical model can be computed as:

$$\Delta P = \sum_{n=1}^{N_b} (P_{bn} - P_{pn}) \tag{10}$$

Where P_{bn} are the pump powers calculated by the analytical model and P_{pn} are the pump powers only taking into account the loss due to attenuation and neglecting the interactions between pumps.

For each distance along the fiber the optical power difference was computed. If the difference was positive, that means the analytical model calculates more energy than total energy in the optical fiber, so the energy calculated on the model was decreased by ΔP being distributed for each pump, proportional to the total power of them. That was considered because the pumps with more power tend to interact more between them. If the difference was negative, the pumps energy were increased by the same criteria.

III. RESULTS

Fig. 3 shows the analytical and numerical model results of the signal gain for a WDM distributed amplifier with eight signals located in the C-band amplified by three optical pumps. The amplification occurs in a 50 km optical fiber with the parameters used for a standard Corning SMF fiber. The input power is -20 dBm per channel.

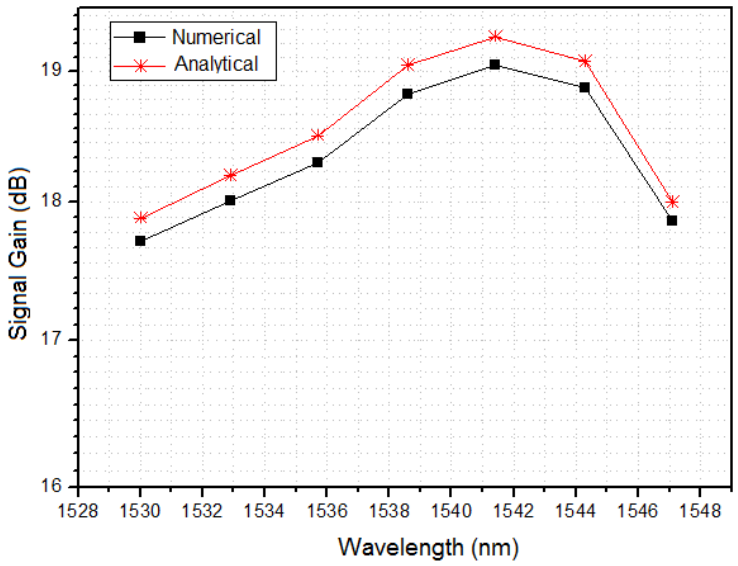

Fig. 3. Signal gain for eight channels over the C-band for a 50 km SMF optical fiber amplified by three optical pumps.

The three optical pumps wavelengths were 1430 nm, 1438 nm e 1446 nm with 200 mW of power each. The distributed optical amplifier was applied in a SMF optical fiber with a total length of 50 km. Fig. 3 shows a good agreement between the numerical and analytical model in that case. For this

  ISSN 2179-1074

http://dx.doi.org/10.1590/2179-10742016v15i3612

configuration the entire amplification of the C band is not cover with an amplification band of 18 nm.

However, when the number of pumps is increased, with the purpose of amplifying the C+L optical bandwidth, the discrepancy between analytical and numerical models increases considerably. The amplification of most part of the L-band signals occurs due to second order pumps, i.e., pumps that were amplified by other pumps [11]. Therefore the interaction between pumps is more critical in that scenario and is responsible for this discrepancy.

Fig. 4 shows the results for a system with eight pumps with parameters showed in table 1 found in the bibliography [12]. The link had a length of 80 km allowing the second order amplification to occur.

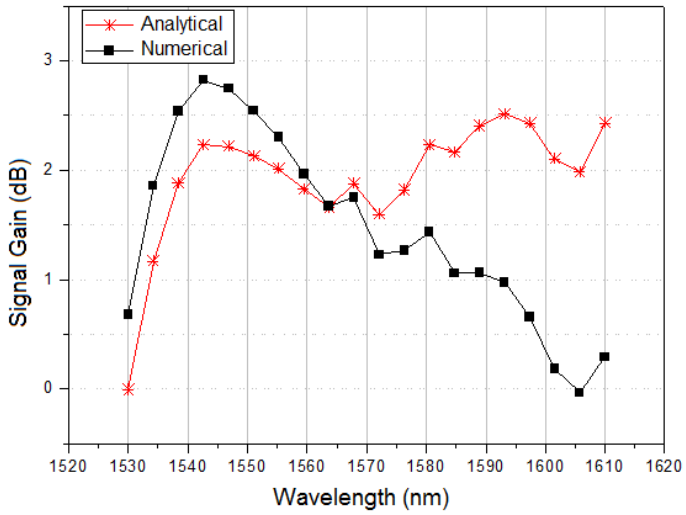

Fig. 4. Signal gain as a function of the wavelength signal for eight pump lasers in 80 km of SMF optical fiber.

It can be seen that from the L band, above 1560 nm, a significant discrepancy between the numerical and analytical model happens. This behavior arises because the pumps with higher wavelengths have less power initially, so they are amplified by the other pumps and after that, when their levels are high enough, they will be responsible for amplifying the L-band, increasing the error in this spectrum region.

TABLE I. PUMP WAVELENGTHS AND THEIR RESPECTIVE POWERS [12].

Wavelength (nm)	Power (mW)	Wavelength (nm)	Power (mW)
1425,0	125,0	1461	65,0
1432,5	105,0	1472	34,5
1440,0	105,0	1489	34,0
1450,0	82,5	1508	34,0

For this reason, the energy conservation analysis becomes important as can be seen in Fig. 5. The result depicts the difference, as function of the distance, between the total energy computed by the analytical model and the conservation energy assumption taking into account the optical pumps only propagating along the optical fiber.

  ISSN 2179-1074

http://dx.doi.org/10.1590/2179-10742016v15i3612

To solve this limitation of the analytical model, a correction analysis was made over the difference between the energy of the pumps only propagating and the pumps interacting. Figure 6 shows the result with the corrected model for the same configuration as in Fig.4.

The response difference between the corrected and the analytical model decreases with the wavelength due to the energy redistribution that happens more in higher wavelengths which suffer more with the simplifications of the analytical model. When eight optical pumps are used, the pump at 1508 nm for instance will suffers more with the depletion of his power by the optical signals into the C+L band, so the impact of his correction will be more observed in higher signal wavelengths, around 1608 nm in this case.

It may be observed that, after the correction was applied, the gain profiles of the numerical model and the corrected analytical model show the same behavior, with a relatively small error. The difference varies around 1 dB for wavelengths in the C-band, up to ~1560 nm. The best result of the corrected model, however, occurs for the L-band. This is reasonable, since the signals in this band are mostly amplified by second order Stokes waves. This is the energy transferred from a pump in the beginning of the band (14xx nm) to another pump, whose wavelength is higher than the first. Subsequently, it is transferred to the signal. This type of behavior increases even more the discrepancy in the gain values, because the analytical model does not consider in its first iteration part of the interaction between the pumps.

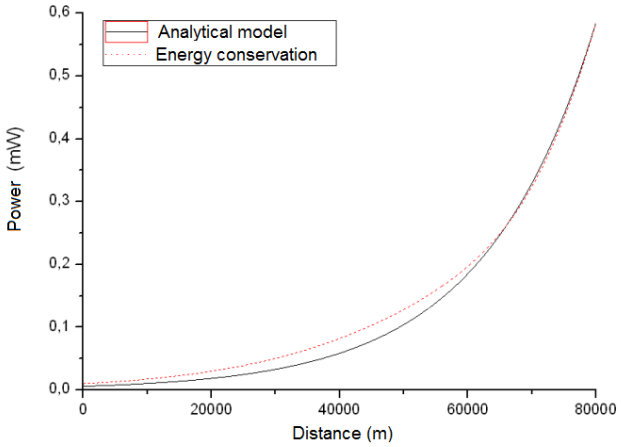

Fig.5. Total pump power as a function of distance for the original analytical model and the model with the correction corresponding to energy conservation.

  ISSN 2179-1074

http://dx.doi.org/10.1590/2179-10742016v15i3612

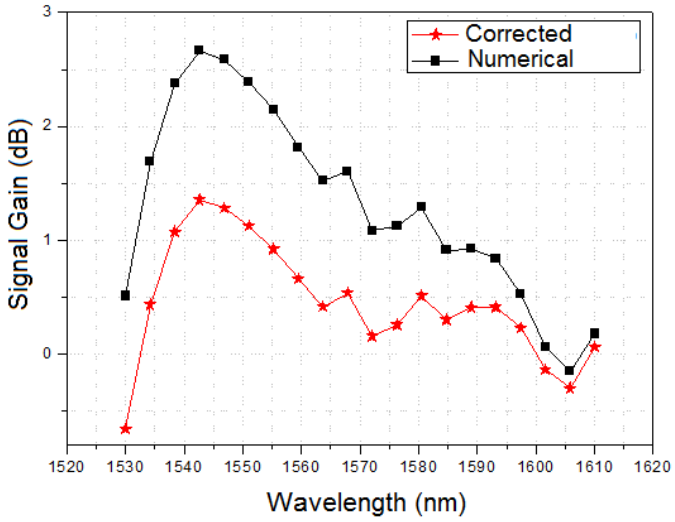

Fig. 6. Signal gain for the numerical model and the corrected analytical model for 8 pump lasers in 80 km of SMF.

Figure 7 shows the gain as a function of the wavelength of the WDM channels for a distributed Raman amplifier with 50 km of SMF. In this case, 13 pump lasers were considered whose wavelengths and powers are indicated in table 2, as found in the bibliography [13].

TABLE 2: PUMP WAVELENGTHS AND THEIR RESPECTIVE POWERS [13].

Wavelength (nm)	Power (mW)	Wavelength (nm)	Power (mW)
1410,8	107	1455,8	42
1417,5	107	1466,0	38
1424,2	110	1473,2	27
1431,0	74	1480,5	24
1437,9	55	1478,0	40
1444,8	44	1510,3	60
1451,8	44		

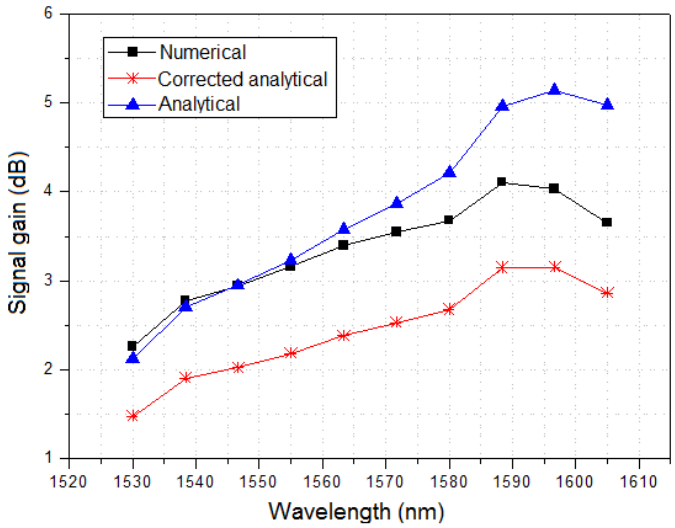

Fig. 7: Signal gain for 13 pump lasers in 50 km of SMF.

  ISSN 2179-1074

http://dx.doi.org/10.1590/2179-10742016v15i3612

As can be seen in Fig. 7, from 1555 nm on, the gain values obtained with the numerical and analytical models differ, since at higher wavelengths the signals are amplified by second order Stokes waves.

Also, it can be seen that the difference between the gain of the numerical model and the analytical model varies considerably throughout the wavelengths. With the correction, however, this difference shows a better steadiness throughout the signal wavelengths, which leads to a trustier analysis in terms of ripple. The difference between the corrected model and the analytical model is more constant in this case because the larger number of pumps is responsible to more pump-pump interactions and to maintain more pumps with significant power along the fiber length.

It should be noted that, in general, there is no reduction of the error between the analytical and numerical models, but rather the curve adapts better to the shape of the result of the numerical model. This leads to a better evaluation of the influence of the ripple and their application in optimization algorithms for ripple metrics. The corrected model can be applied for any pump configuration but the difference for the analytical model will show advantage and will approach to the numerical model only with the increase of optical pumps to cover a larger bandwidth.

IV. CONCLUSIONS

In this work, corrections were discussed, from the perspective of energy conservation, to improve the performance of an analytical model for L-band and considering a large number of pump lasers.

The numerical model for analyzing the behavior of Raman amplifiers yields a more complete result, seeing as it includes phenomena as double Rayleigh scattering and Raman amplified spontaneous emission.

However, due to computational costs, analytical models based on evolution of pumps become attractive, seeing as, in a significant part of the applications, they present results considerably approximated to the numerical model. One of the approximations in this model assumed that initially some pumps did not interact with each other. On the contrary, it assumed they only propagated without loss of power to other pump lasers with different wavelengths. Analyzing the relation between pumps from the perspective of energy exchange, this approximation violates the conservation of energy principle.

Correcting the evolution of pumps in a way that the energy is conserved yields that the results of the analytical model approximate better those of the numerical model. This is observed mainly for signals in the L-band, which owe their amplification mostly to second order Stokes waves. This, probably, is the main factor which increased the discrepancy from the numerical model to the analytical model.

REFERENCES

[1] S. Singh, A. Singh, R S. Keller, “Performance evaluation of EDFA, Raman and SOA optical amplifier for WDM systems”, Optik, vol. 124, pp. 95-101, 2013.

  ISSN 2179-1074

http://dx.doi.org/10.1590/2179-10742016v15i3612

[2] V. R. Kumbhare. “Raman Amplifier Characteristics with Variation of Signal Power and Pump Power With and Without Amplified Spontaneous Emission”, International Conference on Recent Trends & Advancements in Engineering Technology, 2015.

[3] T. V. N. Coelho, M. J. Pontes, J. P. Carvalho, J. L.Santos, A. Guerreiro. “A Remote Long-Period Grating Sensor with Electrical Interrogation assisted by Raman Amplification.” Optics and Laser Technology, v.47, pg. 107-133, 2013.

[4] M. Fernandez-Vallejo, M. Lopez-Amo. “Optical Fiber Networks for Remote Fiber Optic Sensors.” Sensors (Basel), vol. 12, pp 3929-3951, 2012.

[5] C. R. S. Fludger; V. Handerek, “Pump to signal RIN Transfer in Raman Amplifier”, *Electron. Lett.*, vol. 37, no. 1, pp. 15-17, Jan 2001.

[6] J. Bromage. “Raman Amplification for Fiber Communication System.” *Journal of Lightwave Technology*, vol. 22, no. 1, pp 79-93, Jan 2004.

[7] A. Berntson, S. Popov, E. Vanin, G. Jacobsen, and J. Karlsson, “Polarization dependence and gain tilt of Raman ampplifiers for WDM systems,” In *Proc. Opt. Fiber Commun* (OFC2001), Anaheim, CA, 2001.

[8] Shirley P. N. Cani, L. de Calazans Calmon, M. J. Pontes, M. R. N. Ribeiro, M. E. V. Segatto, e A. V. T. Cartaxo, "An Analytical Approximated Solution for the Gain of Broadband Raman Amplifiers With Multiple Counter-Pumps", *Journal of Lightwave Technology*, vol. 27, no.7, pp. 944-951, 2009.

[9] S. Wang e C. Fan, “Generalised attenuation coefficients and a novel simulation model for Raman fibre amplifiers”, *IEE Proc.-Optoelectron.*, vol. 148, no. 3, pp. 156-159, 2001.

[10] M. N. Islam, “Raman Amplfier For Telecommunications 1. Physical Principles,” *Springer Series in Optical Sciences*, EUA, 2004.

[11] H. Kidorf; K. Rottwitt; M. Nissov; M. Ma; E. Rabarijaona. “Pump interactions in a 100nm bandwidth Raman Amplifier.” *IEEE Photonics Technology Letters*, vol. 11, no. 5 pp. 530-532, 1999.

[12] M. Achtenhagen, T. G. Chang, B. Nyman e A. Hardy, “Analysis of a multiple-pump Raman amplifier”, *Applied Physics Letters*, vol. 78, no. 10, pp. 1322-1324, 2001.

[13] S. Namiki and Y. Emori. “Broadband Raman amplifiers design and practice, “ In *Optical Amplifiers and Their Applications*, OSA Technical Digest Washington DC: Optical Society of America, OMB2. 2000.

Brazilian Microwave and Optoelectronics Society-SBMO *received 10 Mar 2016; for review 17 Mar 2016; accepted 7 July 2016*
Brazilian Society of Electromagnetism-SBMag *ISSN 2179-1074*